Article:
Sinha, S orcid.org/0000-0002-9163-7474 (2017) Transient evolution of suspended and benthic algae in a riverine ecosystem: A numerical study. Ecological Modelling, 348. pp. 78-92. ISSN 0304-3800

https://doi.org/10.1016/j.ecolmodel.2017.01.008

Transient evolution of suspended and benthic algae in a riverine ecosystem: a numerical study

Sumit Sinha[1]

[1] School of Architecture, Geography and Environmental Science, University of Reading, Whiteknights, Reading RG6 6AB, UK

Correspondence to: S. Sinha (sumit.sinha@reading.ac.uk)

Abstract

It is a well-established fact that there is no direct resource competition between pelagic and benthic primary producers when their habitats are located in physically separate areas. However, the benthic habitat located at the bottom of the water column is affected by the light rays that gets attenuated as it passes through the pelagic zone and is obstructed by the algal cells and suspended material present in the water column. Therefore, benthic primary production is very much influenced by the conditions and concentrations in the pelagic zone. Another level of complexity is added to the system while considering the impact of flowing water in a riverine environment. In the research presented here a numerical model is developed to examine the impact of flow and nutrients on pelagic and benthic primary producers. The aforementioned numerical model solves advection diffusion and reaction (ADR) equation through TVD (total variation diminishing) - MacCormack scheme. The diffusion term is solved through central difference scheme. The model results are first validated by comparing the results with analytical solutions for the simplified case. The validated model is then applied to a 30 kms stretch of the Bode River and simulations are conducted for multiple flow conditions. Impact of transient flow and nutrient boundary conditions on the evolution of algal trait is examined. Our simulation exercise highlights the importance of residence time in the temporal evolution of algae in pelagic and benthic zone and further identifies the most sensitive parameter influencing the evolution of the algal community modelled. Our research also reveals that largest uncertainty in the modelling stems from the wide range of entrainment rate that could be used for modelling resuspension of benthic algae in pelagic zone. The use of higher entrainment rate increased the algal concentration in the water column by 48% for identical flow conditions.

Key Words: Pelagic algae, Benthic algae, Eutrophication, Numerical modelling

1 Introduction

Eutrophication leading to algal bloom is one of the most severe ecological and environmental problems for both inland and coastal water bodies (Chun et al. 2007, David et al. 2010, Heisler 2008, Simon et al. 2010). Increased frequency of algal blooms is detrimental to economic and recreational pursuits, human and aquatic ecosystems in general (Muttil and Lee 2005). One of the major issues associated with algal bloom is depletion of dissolved oxygen and creation of hypoxic zone (Cox 2003). The hypoxic zone thus created has a destabilizing impact on the fish habitat in the surface waters. Beyond a certain threshold value algae can also lead to occasional human poisoning through intake of contaminated food sources (Huppert et al. 2008, Alan et al. 2005). It has been established that algal blooms are primarily caused by some combination of climatic conditions, nutrient concentrations in surface waters and critical hydrodynamic conditions. The problem of understanding the physics behind the algal bloom is further exacerbated by algal traits, benthic and suspended/pelagic algae, which are located in physically separate areas. Bottom attached benthic algae observed in the range of 100 – 150 mg chlorophyll-a have been deemed unacceptable for river recreation (Welch et al. 1998; Suplee et al. 2009). Elevated level of benthic algae also is also detrimental for tourism and business (Pretty et al. 2002, Dodds et al. 2009). Increased agricultural activity in the wake of green revolution at the starting of twentieth century, combined with excessive use of fertilizers and manure has led to increase nutrient concentration in streams flowing through agricultural and urban areas (Smil 1999, Spaulding and Exner 1993). Multiple researchers have examined the dynamics of algal bloom from hydrodynamic and eutrophication point of view (Dodds et al. 2002, Yamamoto et al. 2002, Mitrovic et al. 2003, Gao et al. 2007). However, most of these studies are either experimental or statistical in nature based on the observed data. Although, of inherently sound scientific value, the observed data for bottom attached algae is usually studied for low flow conditions and shallow streams that fails to disentangle the impact of changing

flow conditions on the dynamics of benthic algae. The spatiotemporal evolution of suspended and benthic algae under transient flow and nutrient boundary conditions in aquatic environment is a tightly coupled and a highly non-linear phenomenon. The problem of tracking the evolution of different algal trait is compounded further by the asymmetric competition for light and nutrients across habitat boundary in shallow aquatic ecosystems by benthic and pelagic primary producers (Jager et al. 2014). In a shallow aquatic ecosystems light that is supplied from above first passes through suspended algae where it gets attenuated by the presence of dissolved substance and suspended particles, consequently the benthic primary producers are distinctly influenced by attenuation of the light coming from the top (Kirk 1994, Vadenboncoeur et al. 2001). In contrast nutrients are usually released and supplied from the river bed. It is a well-known fact that particulate nutrients accumulate in sediments which are eventually released back in the water column (Rizzo et al. 1992, Caraco et al. 1992). The transfer of nutrients from the bottom of the river can be hampered by the production of benthic algae. This cyclical connection and asymmetric competition for resources makes a unique and interesting setting for examining the evolution of benthic and suspended algae under varying flow, nutrients and light conditions. Furthermore, algal cells are of higher specific density than water, consequently they sink out of the pelagic zone and part of their nutrient content is mineralized in the sediment layer (Jager et al. 2010). It is the hydrodynamic entrainment rate near the bed, varying with the flow condition, combined with turbulent mixing in the vertical direction is then responsible to get the nutrient back into the water column. Although the importance of the impact of fluvial processes (shear velocity, water depth, surface width and flow velocity) on spatial and temporal dynamics of algal biomass is well recognized in the lake research community (Riley et al. 1949; Sverdrup et al. 1953; Anita 2005; Peterson et al. 2005), an equivalent study in a riverine environment is somewhat missing. To quote, Nijboer and Verdenschot (2004), “models are needed for forecasting the effect of eutrophication on stream and river ecosystems”. In recent

years with concomitant advances in computing power and numerical methodology there has been a renewed interest in understanding and disentangling the various effects of physical processes on biological variables.

The main objective of the research presented in this paper is to examine the spatiotemporal evolution of suspended and benthic algae in river reach under transient flow and nutrient boundary concentrations. Furthermore, we also examine the impact of changing light conditions as well as loss/death rate of both suspended and benthic algae on the temporal evolution of both suspended and benthic algae. In order to accomplish the aforementioned objective we developed a computationally efficient numerical model to solve Advcection Dispersion Reaction (ADR) equation in a channel with linear as well as non-linear decay term. Simulation results were validated against the analytical solution where present. The validated model was than enhanced to include various terms that represent the impact of light and nutrients on the pertinent state variables. The fully developed model is then applied to a 30 kms stretch of the Bode River located in central Germany. Numerical simulations were conducted for a period of 48 hrs to examine the impact of changing light penetration and death rate of suspended and benthic algae on the spatiotemporal evolution of algal traits under different flow conditions.

This remainder of the paper is organized as follows. In section 2 the conceptual framework along with numerical scheme behind the developed model is presented. The model is validated, where possible, with the help of analytical solution at the end of section 2. Section 3 provides the details about the field site and the river reach where the developed hydro-ecological model is applied. The relationship between the major fluvial variables for the reach under consideration is obtained via setup and application of HEC-RAS model, the details of which are provided in section 3. Spatiotemporal evolution of suspended and benthic algae as obtained

by the application of the developed hydro-ecological model is presented in the section 4. The model is developed in FORTRAN-90 and is highly modular in nature for future developments.

2 Method

2.1 Hydro-Ecological Model

The hydro-ecological model developed and presented in this study numerically resolves suspended and benthic algae along with nutrients in a given river reach. Water column is divided into separate suspended/pelagic and benthic zones and spatiotemporal evolution of algae along with nutrients in surface waters and benthic zone is modelled by a mix of partial and ordinary differential equations (ODE) as shown in Eqs. (1) to (4).

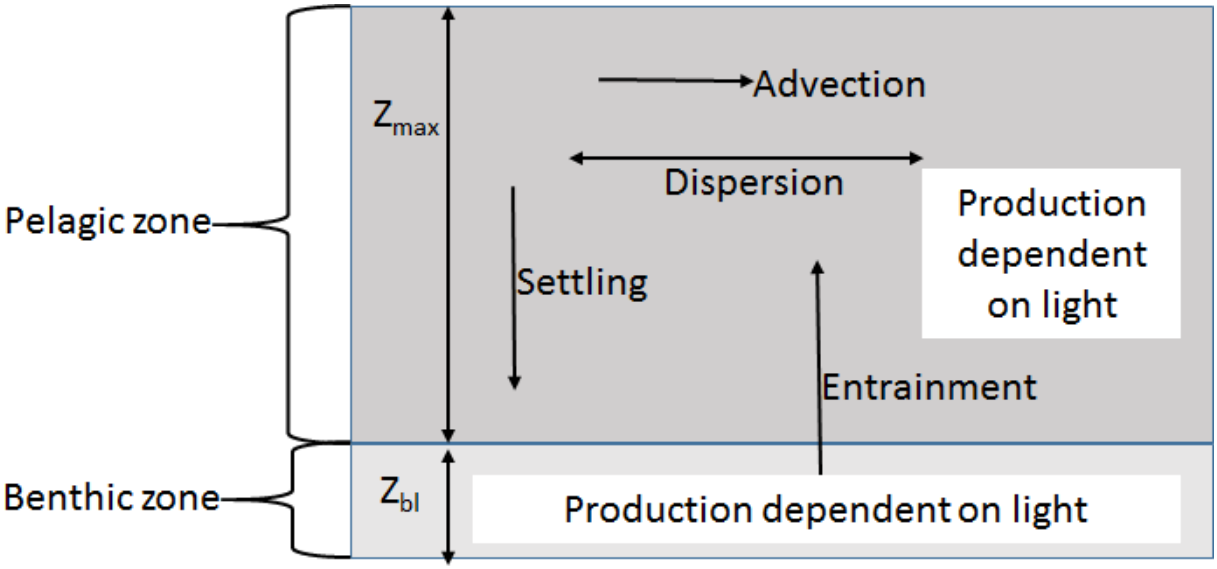

Fig. 1. Schematic of major processes affecting pelagic/suspended and benthic algae

The model is one-dimensional in nature and is extended from Jager and Diehl (2014), developed for lake ecosystems, to account for advection and longitudinal dispersion of suspended algae and nutrients in a river reach. The flow velocity in the domain is denoted by v (ms^{-1}) and longitudinal dispersion D_x(m^2s^{-1}). The biomass of suspended and benthic algae is denoted by A (mg of Carbon m^{-3}) and B (mgC m^{-3}) respectively. Reaction kinetics affecting the

spatiotemporal evolution of suspended algae (A) can be classified broadly either as a source or a sink term for suspended algae. Growth rate, second term on the right hand side (rhs) of Eq. 1, and entrainment of benthic algae from benthic zone to the suspended zone, modelled by the third term on the rhs of Eq. (1), are the two source terms. The loss of suspended algae due to death rate, potentially attributed to grazing, and sedimentation or settling of the suspended algae are the two sink terms and are modelled by third and fourth term on the rhs of Eq. (1) respectively.

$$\frac{\partial A}{\partial t} + v\frac{\partial A}{\partial x} = D_x\frac{\partial^2 A}{\partial x^2} + \frac{A}{Z_{max}}\int_0^{Z_{max}} P_A\left(I(z), R_{surf}\right)dz + \frac{E}{Z_{max}}u_* B - l_A \cdot A - Sed_{rt} A \quad (1)$$

$$\frac{dB}{dt} = BP_B\left(I(z_{max}), R_{bl}, K_B\right) + \Gamma . Sed_{rt} Z_{max} A - l_B \cdot B - Eu_* . B \quad (2)$$

$$\frac{\partial R_{surf}}{\partial t} + v\frac{\partial R_{surf}}{\partial x} = D_x\frac{\partial^2 R_{surf}}{\partial x^2} + \frac{a_{bl}}{Z_{max}}\left(R_{bl} - R_{surf}\right) + c_A l_A A - \frac{c_A}{Z_{max}} A\int_0^{Z_{max}} P_A\left(I(z), R_{surf}\right)dz \quad (3)$$

$$\frac{dR_{bl}}{dt} = -\frac{a_{bl}}{z_{bl}}\left(R_{bl} - R_{surf}\right) - \frac{c_B B}{z_{bl}} P_B\left(I_{z\,max}, R_{bl}, K_B\right) \quad (4)$$

$$P_A\left(I(z), R_{surf}\right) = p_A\frac{I(z)}{I(z) + h_A}\frac{R_{surf}}{R_{surf} + m_A} \quad (5)$$

$$P_B\left(I_{z\,max}, R_{bl}, K_B\right) = p_B\left(1 - \frac{B}{K_B}\right)\frac{I_{z\,max}}{I_{z\,max} + h_B}\frac{R_{bl}}{R_{bl} + m_B} \quad (6)$$

$$I(z) = I_o e^{-(k_A A + k_{bg})z} \quad (7)$$

The growth rate of the suspended algae is affected by the light intensity, which varies along the water column, and is also dependent on nutrient concentration in the surface water as shown in Eq. (5). The zero-order maximum photosynthesis rate for suspended algae is denoted by p_A (day^{-1}). The impact of nutrient concentration and light intensity on the growth rate of suspended algae is modelled via Monod expression (Michaelis and Menten 1913; Michaelis et al. 2011; Monod 1949) which varies between 0 and 1 as shown in Eq. 5. Although phosphorus might not

be the only nutrient of consequence for the growth of suspended algae, nitrate might be equally important, but as the model is applied, detailed in section 3, to the river reach in central Germany and because of the biogeochemical patterns reported by Kamjunke et al., (2014) the control exerted by phosphorus on the growth rate is retained. In Eq. (5) R_{surf} (mg of P m^{-3}) is the total phosphorus concentration and m_A (mg P m^{-3}) denotes the half saturation constant for nutrient limited production rate of suspended algae. The variation of light along the water column depth is modelled according to the Beer-Lambert law (Chapra 2008) and is shown in Eq. (7). Impact of self-shading of suspended algae is incorporated through light attenuation coefficient denoted by K_A (m^2 mg^{-1} C), K_{bg} (m^{-1}) is the background light extinction coefficient attributed to water and colour and I_o (micro-mol photons m^{-2} sec^{-1}) is the light intensity at the water surface. The emigration rate or the detachment rate of bottom attached benthic algae is modelled as the function of shear velocity (u_*) and an empirical constant E after Graba et al. (2010). The depth of water column, zone of suspended algae, is denoted by Z_{max}(m). Sedimentation and death/loss rate of suspended algae is denoted by Sed_{rt} (m^{-1}) and l_A (m^{-1}) respectively. The temporal evolution of benthic algae is modelled via ordinary differential equation shown in Eq. (2), the production rate, first term on the rhs of Eq. (2) and the sedimentation rate of suspended algae, second term on rhs of Eq. (2), are the two source terms for the benthic algae. Production rate of benthic algae, as shown in Eq. 6, is modelled as a first order-logistic model, p_B(day^{-1}) is the maximum photosynthesis rate and K_B (mg C m^{-2}) is the theoretical maximum carrying capacity under given condition. Production rate is further affected by the light intensity reaching the river bottom (I_{zmax}) which obtained through the Beer-Lambert law as explained before and nutrient limitation arising from the concentration of phosphorus in the benthic layer which is again modelled via Monod expression. Total concentration of phosphorus in the benthic layer is denoted by R_{bl} (mg P m^{-3}) and m_B (mg P m^{-3}) denotes the half saturation constant for nutrient limited production rate of benthic algae. A

fraction (Γ) of settling suspended algae attaches itself to the benthic algae and acts as a source term for the benthic algae. The loss of benthic algae attributed to respiration/excretion, sloughing, grazing etc. (Flynn et al. 2013) is modelled through first-order rate coefficient l_B (day^{-1}), third term on the rhs of Eq. 2. Furthermore, the emigration of benthic algae, last term on the rhs of Eq. (2), due to the shear exerted by the flowing water acts as a sink for benthic algae but a source for suspended algae as explained before. The contrasting nature spatiotemporal evolution of nutrients in surface water (R_{surf}) in comparison to suspended algae is revealed by the fact that the source and sink term for the suspended algae act in opposite manner for surface nutrients as shown by third and fourth term on the rhs of Eq.(3). These terms are multiplied by the appropriate conversion constant i.e. C_A and C_B in Eq. (3) and (4) that represents phosphorus to carbon ratio of suspended and benthic algae (R_{bl}). The second term on the rhs of Eq. (3) models the nutrient exchange between the benthic zone and the water column. The exchange rate of nutrients between benthic zone and the water column is denoted by a_{bl} ($m\ day^{-1}$) and is contingent on the comparative concentration of nutrients in benthic zone and the water column. The temporal evolution of nutrients in benthic zone (R_{bl}) is modelled with the ODE shown in Eq. (4), once again the source term for benthic algae (B) act as a sink term for benthic nutrients as shown by the second term on the rhs of Eq. (4). The thickness of benthic layer is denoted by z_{bl}. The first term on the rhs of Eq. (4) models the exchange dynamics of nutrients between benthic zone and the overlying water column, please note that this term can change from source to sink and back depending on the comparative concentration of nutrients in water column and the benthic zone.

2.2 Numerical Scheme

The governing equations for suspended algae and surface nutrients, Eqs (1) and (3), describing the spatiotemporal evolution of algae and nutrients in riverine ecosystems are essentially Advection-Dispersion-Reaction (ADR) equations. Advection, dispersion and reaction (ADR) are the fundamental processes depicting the transport of solute within a water body. In this section we present detail description of the numerical methods used for the resolution of the ADR equations described in detail in section 2.1. As far as the numerical solution of ADR equation is concerned it is a well-known fact that the numerical resolution of the advective term poses the biggest challenge. This is mainly attributed to the fact that the advection process is represented by hyperbolic equation which accepts the discontinuities, commonly known as shock, in the solution. Application of traditional finite difference scheme in the area of discontinuity where the concentration changes sharply leads to spurious oscillations in the numerical solution. Following the pioneering work of Godunov (1959) substantial progress has been made in the area of shock capturing scheme. One of the major developments in the area of numerical resolution of hyperbolic equation with the help of Godunov-type scheme was accomplished by the introduction of the Total Variation Diminishing (TVD) scheme attributed to Harten (1983). TVD-MacCormack scheme after Liang et al. (2010) was used for the resolution of the advective term in this paper. Furthermore, for the easier implementation and development of the model, operator-splitting technique was used. The basic principle behind operator-splitting technique is to break the complex governing model-equations into number of sub-equations. The advantage of this technique is that the most suitable numerical scheme can be used for each sub-equation. In the present work the diffusion term in the ADR equation is solved using second order central differencing scheme and the advective part is solved with TVD-MacCormack scheme (Liang et al. 2010). Application of central differencing scheme for the diffusive part is straightforward hence its details are not presented here. As regards to the

convective and the reaction term as presented in Eqs (1) and (3), it is implemented in the following manner.

- Step 1: Predictor step

$$C_i^P = C_i^n - [(UC)_i^n - (UC)_{i-1}^n]\frac{\Delta t}{\Delta x} + C_i^n \Delta t \quad (8a)$$

- Step2: Corrector step

$$C_i^c = 0.5 * \left\{C_i^p + C_i^n - \left[(UC)_{i+1}^p - (UC)_i^p\right]\frac{\Delta t}{\Delta x} + C_i^p \Delta t\right\} \quad (8b)$$

- Step3: TVD step

$$C_i^{n+1} = C_i^c + [G(r_i^+) + G(r_{i+1}^-)].\Delta(C)_{i+1/2}^n - [G(r_{i-1}^+) + G(r_i^-)].\Delta(C)_{i-1/2}^n \quad (8c)$$

In the equation (8) the superscript p denotes the predictor step, corrector is denoted by the superscript c, the present time level is denoted by the superscript n and the next time level is n+1. The spatial index for the current cell is denoted by the letter i, Δx and Δt denotes the grid size and time step. The value of function G and its argument r is defined as follows

$$\Delta(C)_{i+1/2}^n = (C)_{i+1}^n - (C)_i^n \quad (9)$$

$$r_i^+ = \frac{\Delta(C)_{i-1/2}^n}{\Delta(C)_{i+1/2}^n},\ r_i^- = \frac{\Delta(C)_{i+1/2}^n}{\Delta(C)_{i-1/2}^n} \quad (10)$$

$$G(r_i) = 0.5\psi_i[1 - \phi(r_i)] \quad (11)$$

Ψ_i is dependent on the local courant number and is given by the following equation.

$$\psi_i = \begin{cases} Cr_i(1 - Cr_i), & Cr_i \leq 0.5 \\ 0.25, & Cr_i > 0.5 \end{cases} with\ Cr_i = |U_i|.\Delta t/\Delta x \quad (12)$$

$\Phi(r_i)$ in the equation (11) is a minmod flux limiter which is given by the following expression for this study.

$$\phi(r_i) = max\left(0, \min(2r_i, 1)\right) \quad (13)$$

The drawback with operator-splitting methodology is that only one operator acts on the data at the correct time level (Valocchi et al. 1992). This might lead to inaccurate numerical solution, to circumvent this problem the sequence of application of advection and diffusion solver was changed at every alternate time step. If the advection operator is denoted by L_A and the diffusion operator is denoted by L_D then the sequence of application can be presented by the following expression

$$(C)^{n+2} = L_A L_D L_D L_A (C)^{n+1} \quad (14)$$

As regards to the ODE that governs the evolution of bottom attached benthic algae (B), Eq (2), and benthic nutrients (R_{bl}), Eq (4), is solved by fourth order Runge-Kutta scheme.

2.3 Analytical solution & model validation

The models developed as a part of this research are independently and individually tested and validated against analytical solution if present.

2.3.1 Case 1: Advection Dispersion Reaction (ADR) Equation

In order to verify the accuracy of the numerical model developed, the model is first applied to solve an ADR equation in a channel setting (Fig. 2). ADR equation can be presented as follows.

$$\frac{\partial C}{\partial t} + U \frac{\partial C}{\partial x} = D \frac{\partial^2 C}{\partial x^2} - KC \quad (15)$$

In the above C is the concentration of the tracer in mg/l, U is the velocity in the domain, D is the diffusion coefficient in m^2/s and K is the first order decay rate.

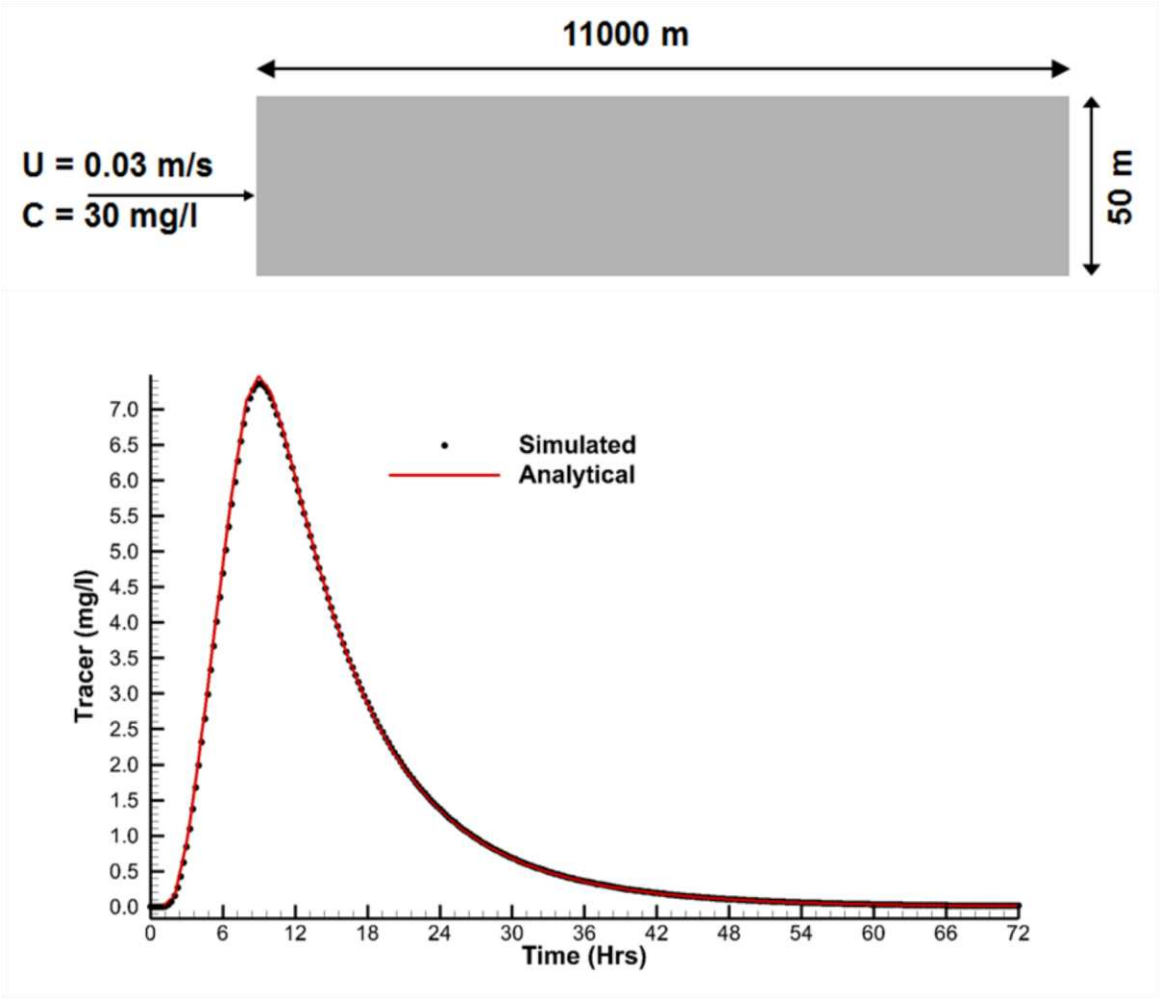

Fig. 2. Comparison between analytical and numerical solution of a passive tracer concentration at X = 2000 m from the upstream end in the middle of the channel

In this benchmark problem flow was simulated in a channel of length 11 km, width 50 m and depth 10 m (Fig. 2). At the upstream end a constant steady discharge of 15 m^3/s was maintained. The downstream boundary condition was prescribed at a constant stage value of 2 m. At the upstream end tracer concentration of 30 mg/l was applied for the first six hours of the simulation. The diffusion coefficient (D) for the tracer was fixed at 30 m^2/s and decay rate K was fixed at 1 day^{-1}. Researchers have frequently used ADR equation as a benchmarking problem for evaluating and assessing their models (Kim et al. 2012; Chao et al. 2008). The analytical solution of the ADR equation in one dimension is given by the following expression as given in Chapra (1997).

$$C(x,t) = \frac{C_o}{2}\left[\exp\left(\frac{U}{2D}(1-\Gamma)\right)\operatorname{erfc}\left(\frac{x - Ut\,\Gamma}{2\sqrt{Dt}}\right) + \exp\left(\frac{U}{2D}(1+\Gamma)\right)\operatorname{erfc}\left(\frac{x + Ut\,\Gamma}{2\sqrt{Dt}}\right)\right] \quad t <= \Gamma$$

$$C(x,t) = \frac{C_o}{2}\left[\begin{array}{l}\exp\left(\frac{U}{2D}(1-\Gamma)\right)\left\{\operatorname{erfc}\left(\frac{x - Ut\,\Gamma}{2\sqrt{Dt}}\right) - \operatorname{erfc}\left(\frac{x - U(t-\tau)\Gamma}{2\sqrt{D(t-\tau)}}\right)\right\} + \\ \exp\left(\frac{U}{2D}(1+\Gamma)\right)\left\{\operatorname{erfc}\left(\frac{x + Ut\,\Gamma}{2\sqrt{Dt}}\right) - \operatorname{erfc}\left(\frac{x + U(t-\tau)\Gamma}{2\sqrt{D(t-\tau)}}\right)\right\}\end{array}\right] \quad t > \Gamma \qquad (16)$$

In the above expression $\Gamma = \sqrt{1 + 4\eta}$ and $\eta = \frac{KD}{U}$. For channel flow problem simulated here $\Gamma = 6$ hrs. After having set up the model the numerical and analytical solution was compared at 2000 m from the upstream end of the domain (Fig. 2) the numerical model was able to reproduce analytical solution in a successful manner.

As mentioned before from the numerical point of view, it is the advective term in the solution of the ADR equation that makes the problem most intractable. In order to test the model's capacity to solve the advective term, the case of pure advection was also considered. To solve the problem of pure advection the above problem is repeated in a slightly different manner. The flow domain/channel was initialized with zero tracer concentration, at the start of the simulation. A constant inflow tracer concentration of 30 mg/l was specified at the upstream boundary, flow velocity in the modelled domain was fixed at a constant value of 0.3 m/s. The comparison between the simulated and analytical tracer concentration at 2000 m from the upstream end of the domain is presented in Fig. 3.

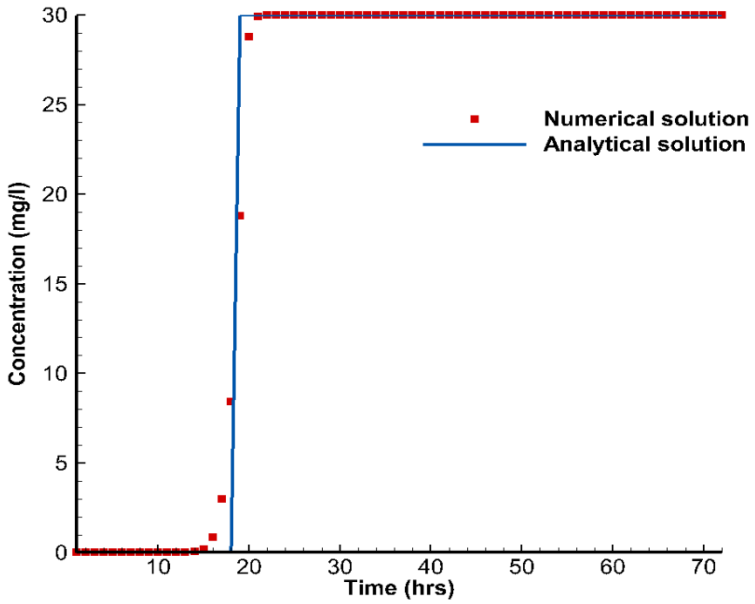

Fig. 3. Comparison between analytical and numerical solution for a tracer pulse at X = 2000 m moving with constant convective velocity of 0.3 m/s

2.3.2 Case 2: ADR Equation with Nonlinear Decay Term

Finally, to test the model and its response to a severe case of stiff source term, we numerically solved advection-dispersion equation with a nonlinear decay term. The reaction term of the source code was modified and the governing equation presented in Eq. (17).

$$\frac{\partial C}{\partial t} + U\frac{\partial C}{\partial x} = D\frac{\partial^2 C}{\partial x^2} - KC^3 \qquad (17)$$

Simulations were conducted in a channel of 3.25 m length, the velocity (U) in the domain was fixed at 0.4 m/s, the longitudinal dispersion (D) was prescribed as 0.3 m^2 s^{-1} and the decay rate (K) was fixed at 0.05 s^{-1}. The initial and the boundary conditions for the considered domain were determined by the analytical solution which is given by the following equation.

$$C(x,t) = \sqrt{\frac{2D}{K}}\frac{2(x - Ut)}{(x - Ut)^2 + 6Dt} \qquad (18)$$

The simulation was conducted in the aforementioned domain for a period of 1.0 second with time step of 0.01 second. The tracer concentration along the channel from the numerical model is compared with the analytical solution at different time step. Good agreement between numerical and analytical solution was obtained as shown in Fig. 4.

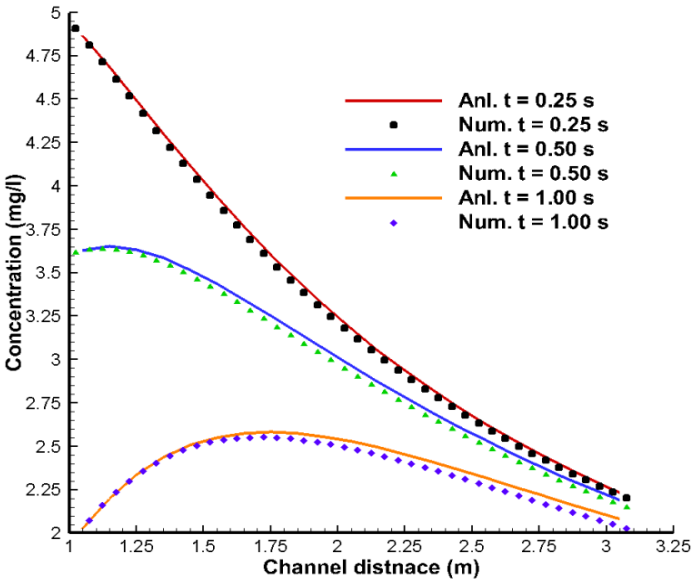

Fig. 4. Comparison between numerical and analytical solution along the channel length at different times

3 Study site and hydraulic modelling

The Bode River basin is approximately 3300 km^2 in area located in central Germany (Fig. 5). The region is characterized by sharp gradients in temperature, precipitation and land use with elevation varying between 55 – 1100 m above mean sea level, the mean annual temperature is 9 ^oC and annual average precipitation is of the order of 660 mm annually with high degree of spatial and temporal variation (450 – 1600 mm; peaks in summer) (Zacharis et al. 2011). The geology of the Bode catchment is dominated by schist and claystone in the one-third of catchment in the high altitude parts and loess soils in the lower area of the catchment. With regard to the land use the catchment is dominated by agriculture amounting to 70% of the total area, urban areas constitute 6 %, open pit mining 1% and rest is occupied by forests. The surveys conducted in order to implement WFD (Water Framework Directive) have found that 76 % of the river bodies in the catchment are unlikely to reach a good ecological status. The adverse water quality conditions found in the surface water within the catchment is potentially attributed to high nutrient loads stemming from agricultural practices as well as modified river morphology. Furthermore, researchers suspect that the current condition might be further exacerbated due to land use change and shift towards the energy plants and increased use of nutrients. In light of above findings, it is imperative to examine and understand the impact nutrient supply on the algal dynamics. With this motivation 30 kms stretch of the Bode River between Hadmersleben and Stassfurt (Fig.5) has been numerically modelled in this research. The aforementioned modelled reach is an ideal stretch for examining the algal dynamics in relation with hydrological variability as the ground water abstraction in the reach is almost negligible and difference between inflow and outflow is less than 3% as found from the observed data

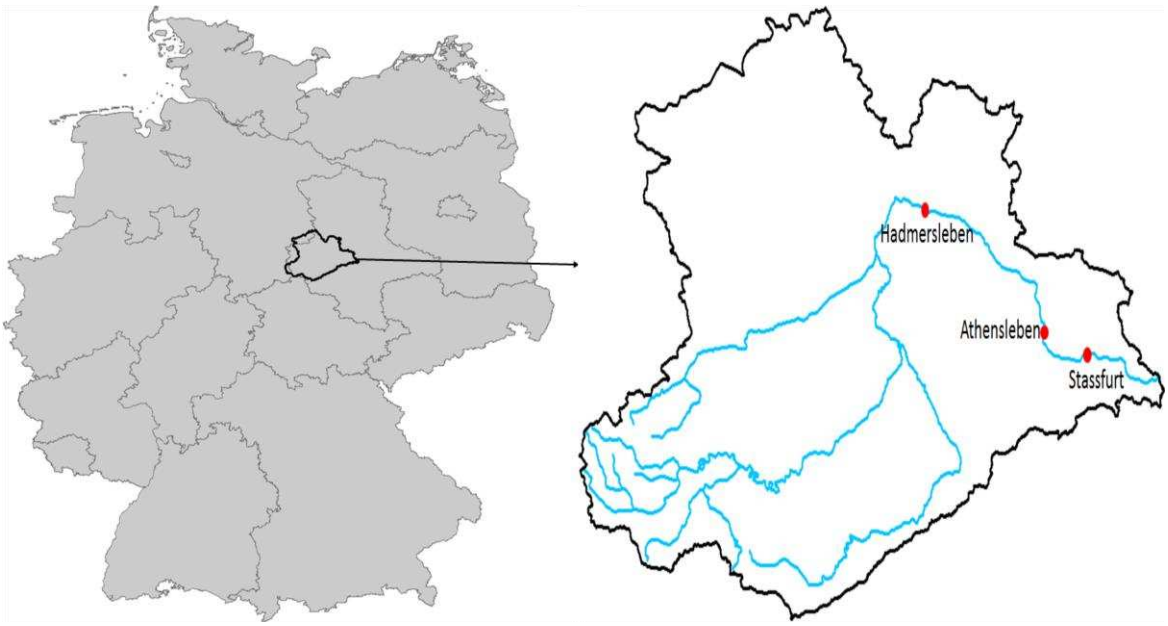

Fig. 5. Bode River basin (right) located in central Germany (left), the modelled river reach runs between Hadmersleben and Stassfurt.

In order to develop relation between primary hydraulic variable, discharge, and ancillary hydraulic variables like, depth-averaged velocity, flow depth, surface width and shear velocity HEC-RAS model (Brunner 2001) was setup for the aforementioned 30 km stretch of the lower Bode River. Four hundred and ten morphological cross-sections were used in setting up the HEC-RAS model for the aforementioned reach between Hadmersleben and Stassfurt and unsteady simulations were conducted. The minimum and maximum flow at Hadmersleben (upstream end) and Stassfurt (downstream end) varied between 2 m^3/s and 72 m^3/s across various simulated flow events. The bed slope for the aforementioned reach along the thalweg is (11/30000). Results from hydraulic simulations were validated with the help of stage observations available at Athensleben, 8 kms upstream of Stassfurt (Fig. 5). The observed variation in the stage was captured satisfactorily by the model (Sinha et al. 2014). Discharge and other ancillary hydraulic variables mentioned before were stored at 15 minutes interval for each morphological cross-section in the HEC-RAS model. Finally, reach-wise representative

values of all the hydraulic variables were obtained at every 15 minutes interval by taking average of these values across 410 morphological cross-sections. The relation between discharge and ancillary hydraulic variables were successfully captured by power-law type of equations (Sinha et al. 2014) as shown in Eq. (19).

$$U = 0.25\,Q^{0.38} \quad (19\ a)$$

$$H = 0.4\,Q^{0.25} \quad (19\ b)$$

$$R = 0.4\,Q^{0.42} \quad (19\ c)$$

$$u_* = 0.0376\ Q^{0.21} \quad (19\ d)$$

$$B = 10.0\,Q^{0.37} \quad (19\ e)$$

In Eq. (19) U is depth-averaged reach-wise velocity, H is the flow depth in the reach, R is the hydraulic radius, u_* is the shear velocity and B is channel surface width. With regards to the longitudinal dispersion (D_x) needed for the solution of suspended algae, Eq (1) and surface nutrients, Eq (3), following formulation (Fishcer, 1966) was used.

$$D_x = \frac{0.011\,UB^2}{Hu_*} \quad (20)$$

4 Simulation results and discussion

We began by reporting the values of ancillary variables for low-flow (2 m^3/s) and high-flow (50 m^3/s) conditions (Table 1). Applying the formulation presented in Eq. (19) we found that the depth-averaged velocity increased by 3.5 times between low and high-flow conditions. The bed shear velocity and longitudinal dispersion values increased approximately by two and ten folds (Table 1). The values of the reported ancillary variables were used by the developed hydro-ecological model for computing the spatiotemporal evolution of suspended and benthic

algae concomitantly with the nutrients residing in the water column as well as the benthic zone (Fig. 1).

Table 1: Values of ancillary hydraulic variables for different flow conditions

Disch. (Q)	Veloc. (U)	Depth(H)	Shear Velocity(u_*)	Surface Width(B)	Longitudinal Dispersion(D_x)
2 m^3/s	0.32 m/s	0.475 m	0.043 m/s	13.0 m	26.47 m^2/s
50 m^3/s	1.11 m/s	1.06 m	0.085 m/s	42.0 m	239.05 m^2/s

It is worth mentioning that benthic algae monitoring programs generally consider shallow or low-flow conditions from the safety point of view of the monitoring personnel (Flynn et al., 2013; Suplee et al., 2012), consequently simultaneous measurements of pelagic and benthic algae for wide range of stream flow conditions is rarely available. Therefore, development and application of numerical models to study the cyclical nature of spatiotemporal evolution of pelagic and benthic algae for range of flow conditions and boundary concentrations is a viable alternative. Hydro-ecological model developed in this research is primarily used to examine the qualitative trends in the evolution of algae and nutrients in pelagic and benthic zone under different boundary conditions for range of parameters values as reported in peer-reviewed published literature.

4.1 Impact of light penetration and decay rate at low-flow conditions for the modelled state variables

The parameter values used by the model along with the initial conditions for the four major state variables i.e. pelagic algae (A_o), suspended nutrients (R_{surfo}), benthic algae (B_o) and benthic nutrients (R_{blo}) is presented in Table 2. The appropriate range for various parameters as reported in literature is also presented in Table 2. As the spatiotemporal evolution of pelagic

algae and surface nutrients are characterised by PDEs presented in Eqs (1) and (3) respectively, Dirichlet boundary condition was applied at the upstream end, Hadmersleben, and Neumann boundary condition at the downstream end, Stassfurt, of the modelled reach (Fig. 5). For the simulation corresponding to low-flow condition the upstream boundary concentration for pelagic algae and suspended nutrients were fixed at 10 mg C m^{-3} and 5 mg P m^{-3} respectively.

Table 2: Parameter values used for hydro-ecological simulation in the Bode River (* parameters which were varied within the specified range)

Parameter	Value	Definition & Unit	Range	Source
a_{bl}	0.05	Nutrient exchange rate between benthic layer and surface water [m day^{-1}]	----	Jager et al. 2014
c_A, c_B	0.02	Phosphor to carbon quota of algae [mg P mg C^{-1}]	----	Jager et al. 2014
h_A, h_B	60	Half sat. const. for light-limited production [µmol photons m^{-2} s^{-1}]	30 – 90	Flynn et al. 2013
I_0	300	Light intensity at the surface [µmol photons m^{-2} s^{-1}]	----	Jager et al. 2014
k_A*	0.03	Light attenuation coefficient due to pelagic algae [m^2 mg C^{-1}]	0.0088 – 0.031	Flynn et al. 2013
k_{bg}*	3.0	Background light attenuation coefficient [m^{-1}]	0.02 – 6.59	Kirk 1994
K_B	1200	Carrying capacity of benthic algae [mg C m^{-2}]	---	Flynn et al. 2013
l_A, l_B*	0.4	Loss rate of pelagic and benthic algae [day^{-1}]	0.0 – 0.8	Flynn et al. 2013
m_A, m_B	90	Half saturation constant for nutrient-limited production [mg P m^{-3}]	5.0 – 175.0	Turner et al.2009
p_A, p_B	1	Maximum production rate pelagic and benthic algae [day^{-1}]	---	Jager et al. 2014
s_A	0.02	Sedimentation rate of pelagic algae [day^{-1}]	0.02 --- 0.2	Long et al. 2011
Γ	0.05	Fraction of settling pelagic algae attaching to benthic zone	----	Jager et al. 2014
z_{bl}	0.01	Depth of the benthic layer [m]	---	Jager et al. 2014
E	0.002	Background emigration rate of benthic algae [s m^{-1} day^{-1}]	0.002 --- 0.004	Labiod et al. 2007; Graba et al. 2013
Ao	250	Biomass of algae in the surface water at t = 0 [mg C m^{-3}]		
Bo	500	Biomass of algae in the benthic layer at t = 0 [mg C m^{-2}]		
R_{blo}	25	Concentration of dissolved nutrients in the benthic layer at t = 0 [mg P m^{-3}]		
R_{surf0}	25	Concentration of dissolved nutrients in the benthic layer at t = 0 [mg P m^{-3}]		

For the specified boundary condition, as mentioned before, we tracked the evolution of benthic algae, benthic nutrients, suspended algae and suspended nutrients at the midpoint of the stream which is 15 kms from the upstream end, Hademersleben, of the modelled domain. Furthermore

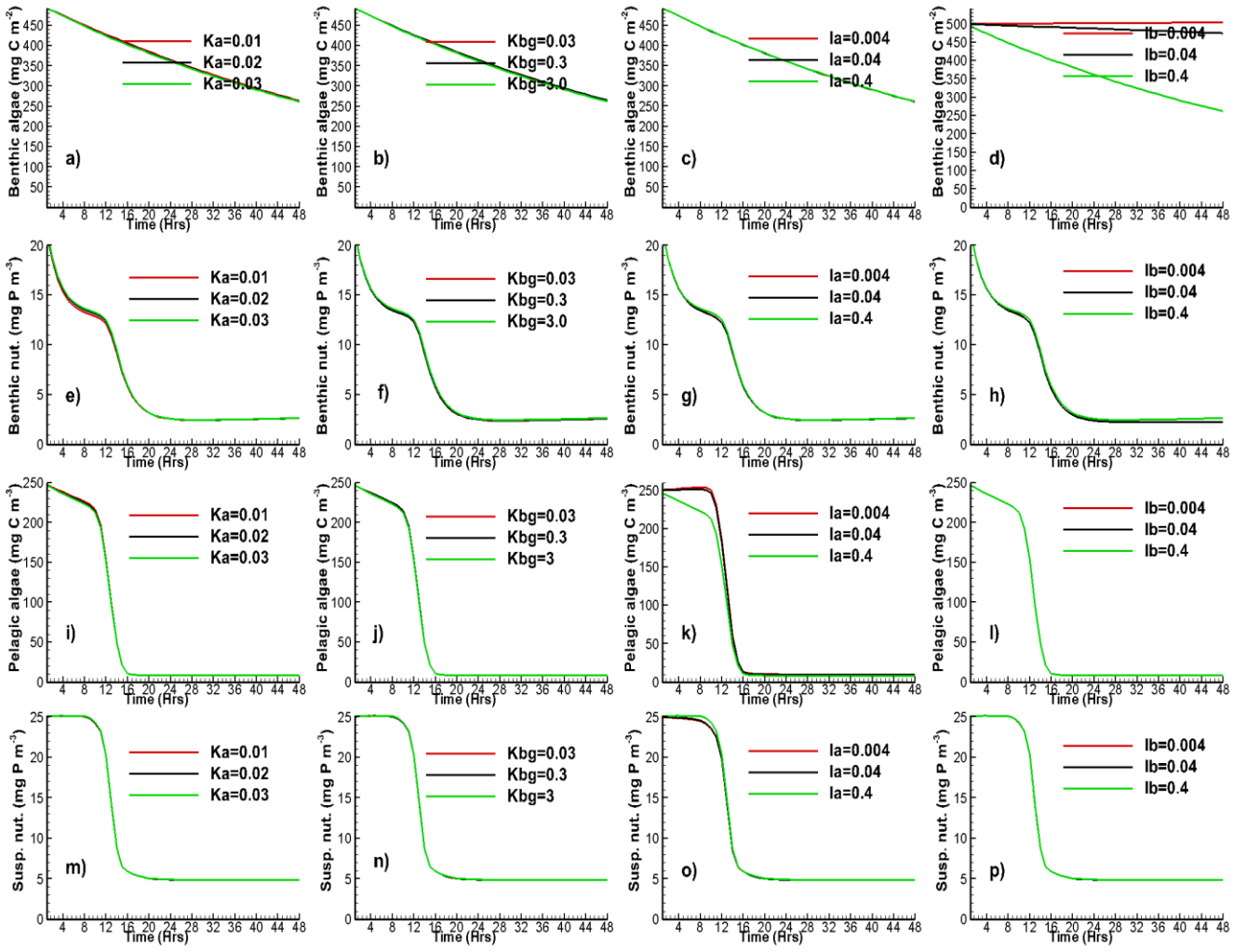

Fig. 6. Variation of benthic algae (a-d), benthic nutrients (e-h), pelagic algae (i-l) and suspended nutrients (m-p) at the midpoint of the stream for inflow of $2 m^3/s$ at benthic algae entrainment rate (E) of 0.002 s m^{-1} day^{-1}

to examine the effect of light penetration (K_a and K_{bg}) and decay rate (la and lb) on suspended and benthic algae, we run multiple simulations by changing the value of the parameters by an order of magnitude within the permissible range where possible. The temporal evolution of benthic nutrients at the midpoint of the stream is presented in Fig. 6 (a-d). The continuous and consistent decrease in the value of benthic algae implies that the sink terms i.e. loss due to decay, third term in the rhs of Eq. (2), and entrainment of benthic algae from benthic to pelagic

zone, last term in the rhs of Eq. (2), dominates the source terms i.e. growth of benthic algae and settling of suspended algae from the water column to the benthic zone. It should also be reiterated that temporal evolution of benthic algae is characterised by the ODE presented in Eq. (2) hence it is not influenced by the boundary conditions, however, the impact of the pelagic algae concentration in the overlying water column is taken in account with the help of the second term in the rhs of Eq. (2). Due to larger impact of the sink terms in this simulation we observed the concentration of benthic algae diminished by 46% from its initial value of 500 mg C m^{-3} to 270 mg C m^{-3}. Furthermore, as we change the value of the parameter K_a, light attenuation coefficient due to pelagic algae, we don't observe any discernible impact on the temporal evolution of the benthic algae (Fig. 6a) within the simulated time frame. To examine the controls of light penetration further, we altered the value of the parameter K_{bg}, background light attenuation coefficient, by an order of magnitude within the specified range (Table 2). Once again we did not observe any distinct difference in the evolution pattern of benthic algae (Fig. 6b). The insensitivity of the parameters associated with light on the evolution of benthic algae can be explained by the fact that the attenuation of the light intensity from the water surface to the bottom of the water column is not significant at low flow and low depth. Furthermore, as shown in Eq. (6) the impact of light is associated with the production term is incorporated in monod kinetic form consequently any change in the intensity of light at the bottom of the water column, benthic zone, results in miniscule change in the growth rate and evolution pattern of benthic algae. Simulations conducted by changing the values of loss rate of pelagic algae (l_a) has no significant impact on the evolution trend of benthic algae (Fig. 6c). As regard to the impact due to change in loss rate of benthic algae (l_b), we observed a significant increase in the depletion of benthic algae, resulting in lower benthic algae concentration at the end of the simulation for the higher l_b values (Fig. 6d). For the l_b value of 0.004 day^{-1} we observed a 0.7 % increase in benthic algae concentration from its initial value of 500 mg C m^{-}

^{3} to 503.67 mg C m^{-3} by the end of simulation period of 48 hrs. As regard to the l_b value of 0.04 day^{-1}, the final benthic algae concentration had decreased by 5.1 % to a value of 474.51 mg C m^{-3}. This distinct impact of loss rate of benthic algae on the evolution trend imply that this is the most sensitive parameter with respect to the temporal evolution of benthic algae. The temporal evolution of the benthic nutrient is presented in Fig. 6(e-h). Benthic nutrients also exhibit a diminishing trend for the entire simulation period. We observed a decrease of 86.5 % in benthic nutrient concentration from its initial value of 20 mg P m^{-3} to 2.3 mg P m^{-3}at the end of the simulation. The contrasting nature of the ODEs governing the temporal evolution of benthic nutrients and benthic algae is worth reiterating, the source term associated with the production rate of benthic algae, first term on the rhs of Eq. (2) becomes the sink term for the benthic nutrients with appropriate conversion factor, second term on the rhs of Eq. (4). Despite the same starting initial concentration of benthic algae and benthic nutrients at 25 mg C m^{-2} and 25 mg P m^{-3} respectively which nullifies the impact of the first term on the rhs of Eq. (4), the overall diminishing trend of benthic nutrients can be attributed to sink term associated with the production of benthic algae which is further magnified due to the presence of the term z_{bl} (Table 2), the thickness of the benthic zone, in the denominator of the second term on the rhs of Eq. (4). Interestingly we did not observe any change in the evolution pattern of benthic nutrient across multiple simulations with different parameter values (Figs. 6 e-h). We finally tracked the evolution of pelagic algae and suspended nutrients characterised by PDEs in Eqs (1) and (3) at the midpoint of the modelled domain and presented in Figs. (6 i-l) and Figs. (6 m-p) respectively. At low flow conditions the average longitudinal velocity as obtained by the hydraulic modelling is 0.32 m/s (Table 1) which implies that a parcel of water starting at the upstream end of the domain will take nearly 13.2 hrs to reach the middle of the modelled segment hence the residence time for the water parcel for half the stream reach is 13.2 hrs. As regard to the temporal evolution of pelagic algae we observed a gradual decrease in pelagic

algae concentration till 13.2 hrs followed by a sharp drop. The concentration of pelagic finally reaches an asymptotic value of 8.7 mg C m^{-3} which is near the prescribed upstream boundary concentration of 10 mg C m^{-3}. This reveals a very interesting and important fact about the interconnection between physics and kinetics, a parcel of water in a stream segment has time that is limited by its residence-time to be acted upon by various kinetic terms before it gets superimposed by the upstream boundary concentration or flushed down the system. The depletion pattern of pelagic algae until the half-reach residence time, 13.2 hrs, is nearly same across the multiple simulations conducted with different parameter values (Fig. 6 i-l). However, at lower decay rates of pelagic algae (la), for the values of 0.04 and 0.004 day^{-1}, we observed the depletion rate of the pelagic algae to be severely diminished (Fig. 6k), until the half-reach residence time, when the sudden and sharp drop in the concentration of pelagic algae is instigated by the arrival of the water parcel from the upstream end carrying the boundary condition signal. As regard to the temporal evolution of the suspended nutrients in the water column, we did not observe a mark difference in the evolution across the multiple simulations conducted with different parameter values (Fig. 6 m-p). The concentration of suspended nutrients in the water column was constant until the half-reach residence time which implies a balance between the source and sink term acting of the suspended nutrients in the water column (Eq. 3).

The source and sink terms used in the equations (Eqs. 1 and 2) describing the spatiotemporal evolution of pelagic/suspended and benthic algae have been used by multiple researchers in different modelling exercise (Whitehead and Hornberger 1984; Wade et al., 2001; Jager and Diehl 2014; Whitehead et al., 2015) and are pretty well understood along with the permissible parameter ranges. However, there seem to exist a significant uncertainty in the value of the benthic algae entrainment rate (E) as reported in Labiod et al., (2007) and Graba et al., (2013) for the experimental work conducted in the field and lab respectively.

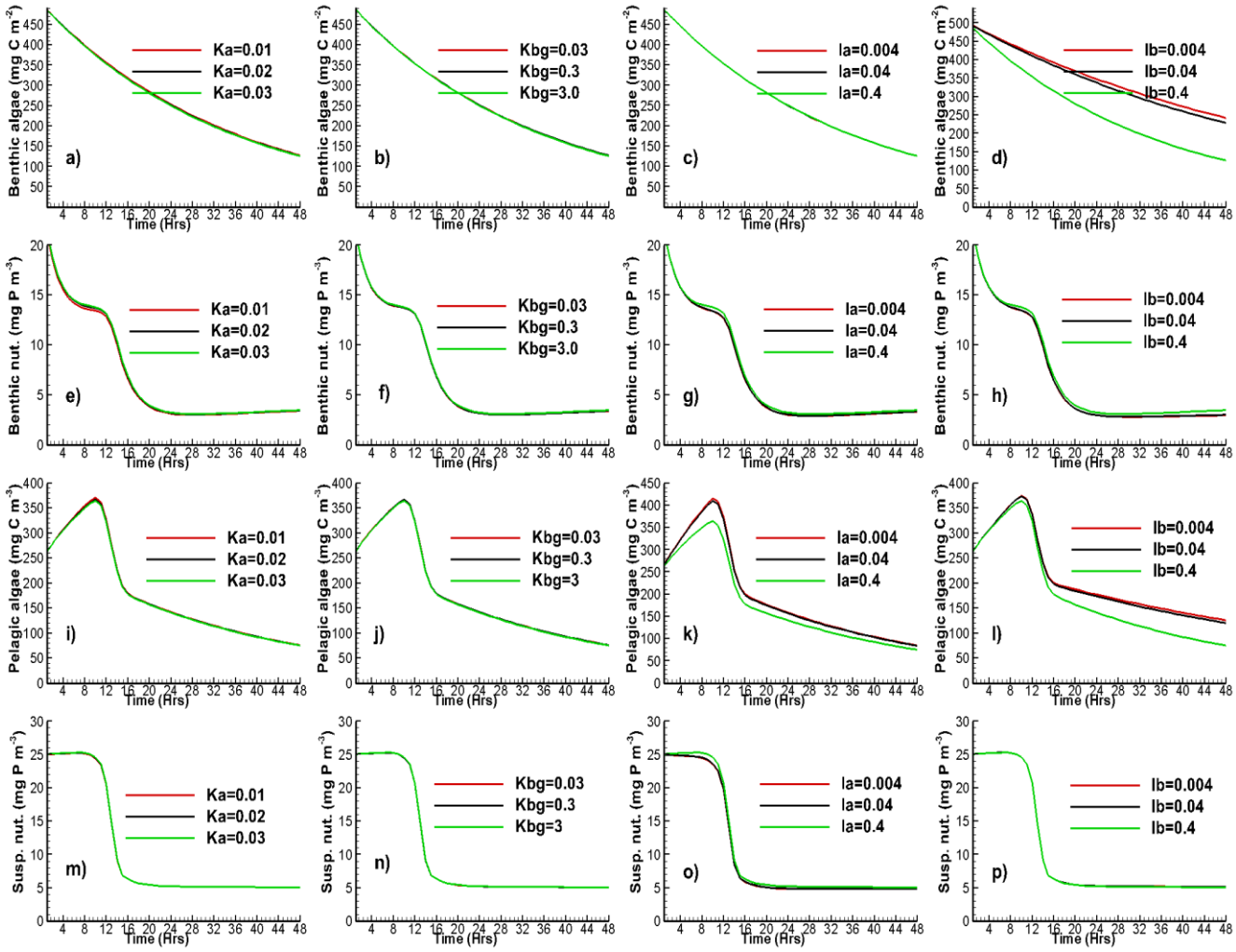

Fig. 7. Variation of benthic algae (a-d), benthic nutrients (e-h), pelagic algae (i-l) and suspended nutrients (m-p) at the midpoint of the stream for inflow of $2 m^3/s$ at benthic algae entrainment rate (E) of 10 s m^{-1} day^{-1}

In order to examine the impact of increased entrainment rate (E), we reran the simulations presented in Fig. 6 with E = 10 s m^{-1} day^{-1} , orders of magnitude larger than our base value of 0.002 s m^{-1} day^{-1} (Table 2). As expected, the increased entrainment rate, resulted in 75% loss, significantly larger than observed for E = 0.002 s m^{-1} day^{-1}at 46 % (Fig 6 a-d), of benthic algae from its initial concentration of 500 mg C m^{-2} to 125 mg C m^{-2}. The depletion trend observed across the multiple simulations conducted with different parameter values are almost identical (Fig. 7 a-d) albeit for the lower values of decay rate of benthic algae (lb). For the values of lb 0.04 and 0.004 day^{-1}, we observed only about 50% reduction in the concentration of benthic algae from its initial concentration. As the entrainment rate (E) doesn't directly figure in the

governing equation for the evolution of benthic nutrients (Eq. 4), we did not observe a mark difference in the evolution pattern of benthic nutrients for the simulations conducted with increased entrainment rate (Fig. 7 e-h). It is interesting to note that because of the increased entrainment of algae from the benthic zone, we observed a bloom of pelagic algae in the water column till half-reach residence time (13.2 hrs) as shown in Figs. (7 i-l). There was nearly 48% increase, to a value of 375 mg C m^{-3} from its initial value of 250 mg C m^{-3}, in the concentration of pelagic algae in the water column until half-reach residence time across the multiple simulations conducted with different parameter values (Fig. 7 i-l). The sharp drop in the concentration of pelagic algae beyond the half-reach residence time is attributed to the upstream boundary concentration. The peak concentration reached for pelagic algae, for la values of 0.04 and 0.004 day^{-1} is even higher at 425 mg C m^{-3} which is expected due to less loss at reduced loss rates. Once again, as the entrainment rate (E), is not present in the governing equation for the spatiotemporal evolution of suspended nutrients in the water column (Eq. 3), we did not observe a significant difference in its evolution pattern (Figs. 7 m-p) when compared with the simulation conducted with entrainment rate (E) value of 0.002 s m^{-1} day^{-1} (Figs. 6 m-p).

4.2 Impact of light penetration and decay rate at high-flow conditions for the modelled state variables

In this section we report the results from the simulations conducted at high-flow rate corresponding to stream discharge of 50 m^3/s which results in average stream-reach velocity and depth values of 1.11 m/s and 1.06 m respectively (Table 1). The shear flow velocity and longitudinal dispersion value at this flow rate was 0.085 m/s and 239.05 m^2/s (Table 1).

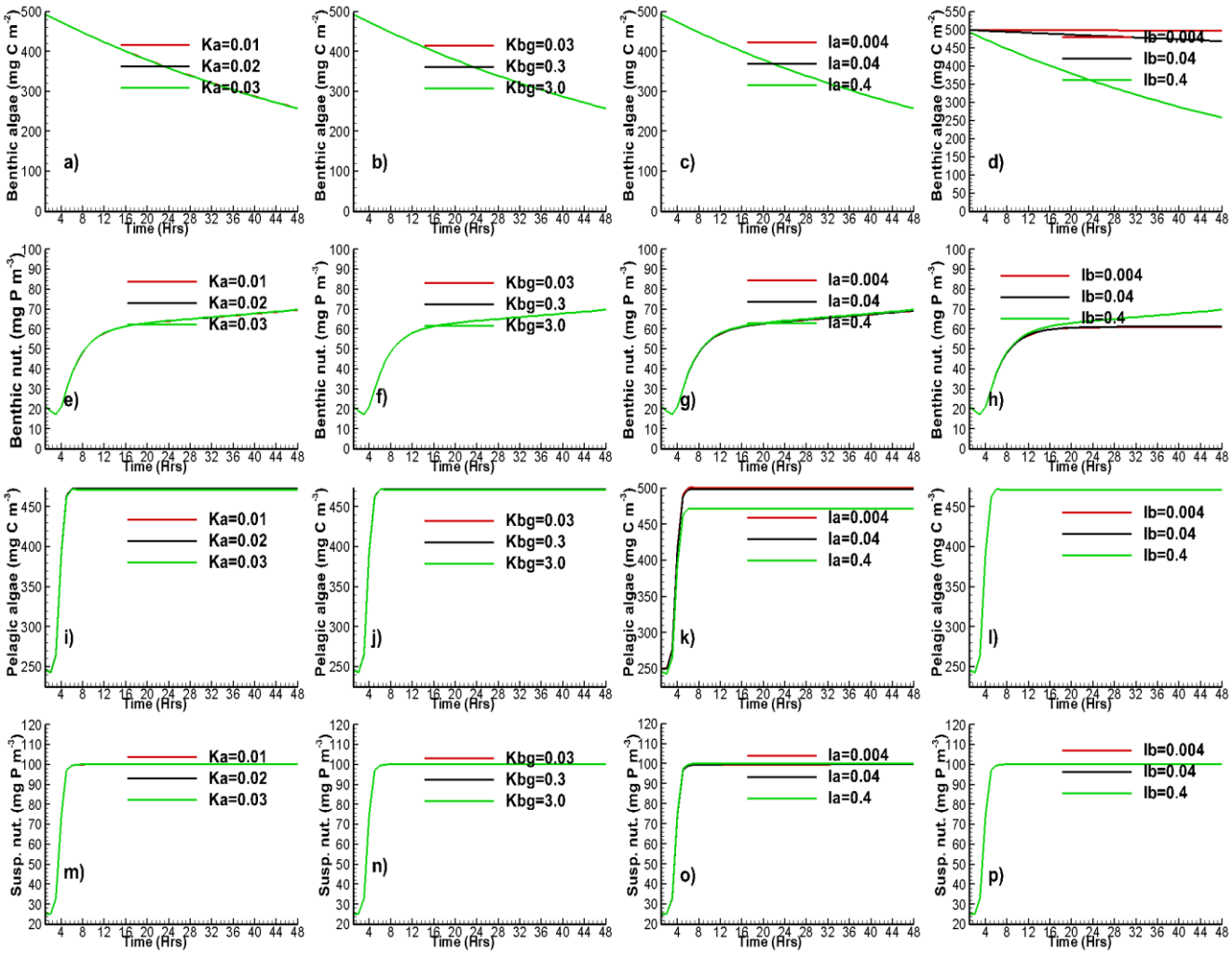

Fig. 8. Variation of benthic algae (a-d), benthic nutrients (e-h), pelagic algae (i-l) and suspended nutrients (m-p) at the midpoint of the stream for inflow of 50m^3/s at benthic algae entrainment rate (E) of 0.002 s m^{-1} day^{-1}

Spatiotemporal evolution of algae and nutrients in pelagic and benthic zone at the midpoint of the modelled reach is presented in Fig. 8. For the aforementioned hydraulic conditions, corresponding to the high flow scenario, the half-reach residence time is 3.75 hrs. The evolution

pattern of benthic algae and the final concentration of benthic algae at the end of the simulated time frame (Fig. 8 a-d) is not very different from the simulations conducted at low flow conditions (Fig. 6 a-d). This can be potentially explained, once again, by the fact that evolution of benthic algae is governed by the ODE (Eq. 2) and is not affected by the upstream boundary concentration. As noted before the most sensitive parameter with regard to the evolution of benthic algae is the loss rate of benthic algae (lb), similar to the low flow conditions (Figs 6d), at lower values of lb i.e. at 0.04 and 0.004 day^{-1}, the final concentration of benthic algae at the end of simulation (Fig. 8d) is significantly greater than in comparison with simulations conducted with other parameter values (Figs. 8 a-c). The nature of evolution of nutrients in benthic zone, Figs. 8 e-h, is very different from what was observed for low flow scenario (Figs. 6 e-h). However, it is worth noting, that until half-reach residence time (3.75 hrs), we observed decreasing trend in the concentration of benthic nutrients, which was reversed thereafter (Figs 8 e-h). This reversal in trend can be explained by the first term on the rhs of Eq. (4), the governing equation for the evolution of nutrients in benthic zone, as the high concentration of surface nutrients from the upstream end reaches the middle of the domain by half-reach residence time, the first term on the rhs of Eq. (4) becomes the source terms which aids in overall increase in the concentration of benthic nutrients. We observed nearly 128% increase in the concentration of benthic nutrients to a value of 67 mg P m^{-3} from its initial value of 25 mg P m^{-3}. It is worth noting that at lower decay rates of benthic algae (lb), specifically for lb values of 0.04 and 0.004 day-1, there is higher concentration of algae in benthic zone (Figs. 8d red and black lines) which leads greater consumption of nutrients from the benthic zone, resulting in lower benthic nutrients concentration (Figs. 8h red and black lines). This trend shows the cyclical and coupled nature of the evolution of benthic algae and nutrients. For the simulations conducted at high flow scenario we hypothesized that a storm-event generating high flow scenarios will generally lead to higher nutrients and pelagic algae concentration from the

upstream reach and terrestrial ecosystem, hence for the high flow conditions we specified the upstream boundary concentration for pelagic algae and nutrients at 500 mg C m^{-3} and 100 mg P m^{-3} respectively. For the aforementioned boundary concentration, the evolution of algae and nutrients in the water column seem to be dominantly governed by upstream boundary concentrations (Figs. 8 i-p).

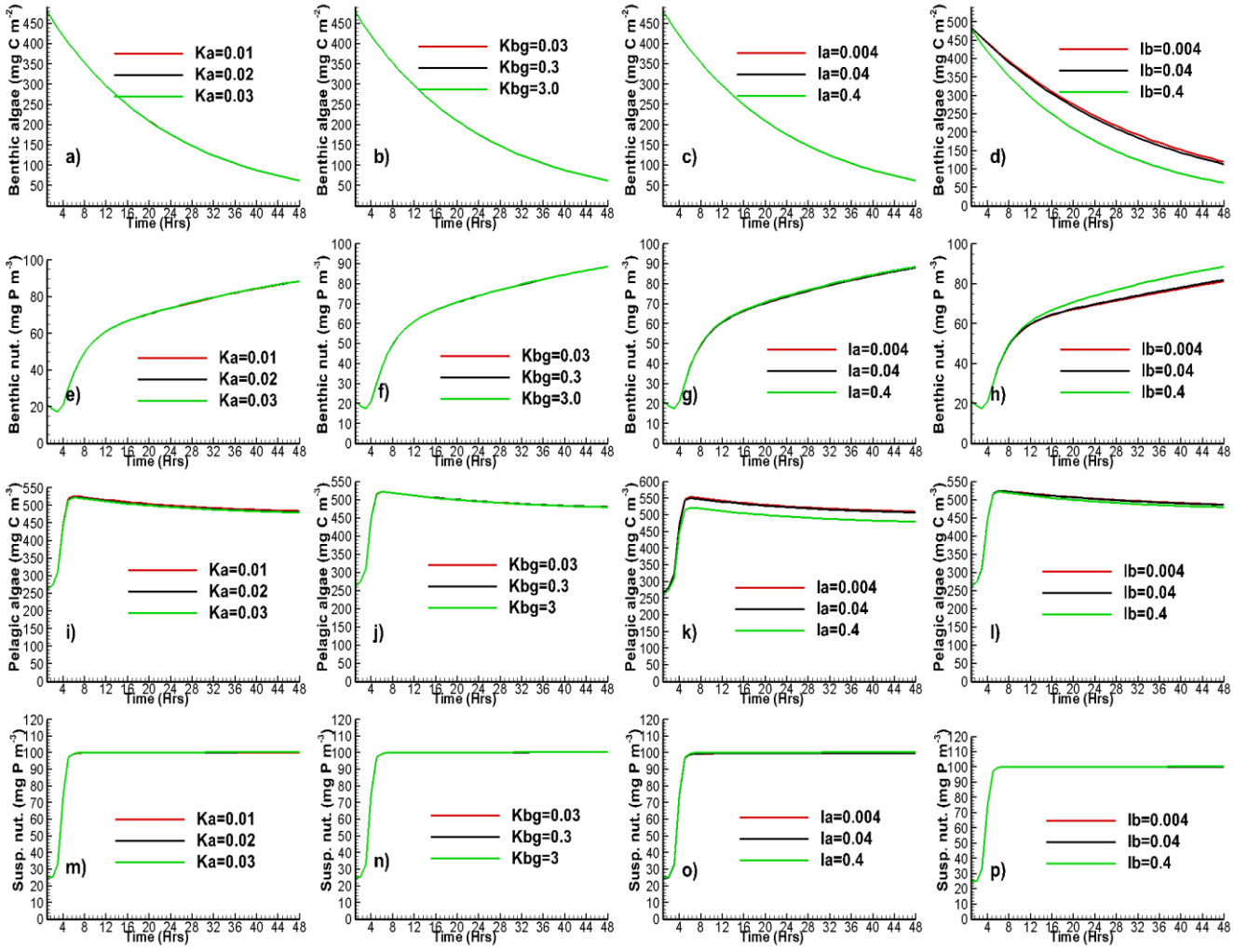

Fig. 9. Variation of benthic algae (a-d), benthic nutrients (e-h), pelagic algae (i-l) and suspended nutrients (m-p) at the midpoint of the stream for inflow of 50m^3/s at benthic algae entrainment rate (E) of 10 s m^{-1} day^{-1}

We finally examined the impact of increased benthic algae entrainment rate (E = 10 s m^{-1} day^{-1}) for high flow condition (Fig. 9). At high entrainment rate the final concentration of benthic algae at the end of the simulation (Figs. 9a-d) is around 67 mg C m^{-2} which is significantly less than the corresponding concentration (125 mg C m^{-2}), at low flow scenario (Figs. 7a-d). This

lower concentration can be explained by the combined effect of the high entrainment rate (E) and higher shear velocity at high flow rate, the product of which acts as the sink term in the evolution of benthic algae as shown in the last term on the rhs of Eq. (2). Once again benthic nutrients shows an increasing trend (Figs 9 e-h) beyond the half-reach residence time which, as explained before, is governed by the upstream boundary concentration of suspended nutrients coming into the system. The higher entrainment rate leads to persistent increase the in the concentration of benthic nutrients for the entire simulation period (Figs. 9 e-h). The evolution of pelagic algae and nutrients in the water column, once again, is dominantly governed by the upstream boundary concentration. However, beyond the half-reach residence time (3.75 hrs), we observed a general decreasing trend in the concentration of pelagic algae (Figs. 9 i-l) which can be potentially explained by the dominance of the sink term associated with the loss rate of pelagic algae (la) as shown by the fourth term in the rhs of Eq. (1). The evolution of nutrients in the water column is primarily governed by the upstream boundary concentration (Figs. 9 m-p).

4.3 Impact of light penetration and decay rate at transient-flow conditions on the modelled state variables

In order to examine the impact of transient boundary conditions, we subjected the modelled domain to synthetic boundary conditions. At the upstream end of the domain we prescribed

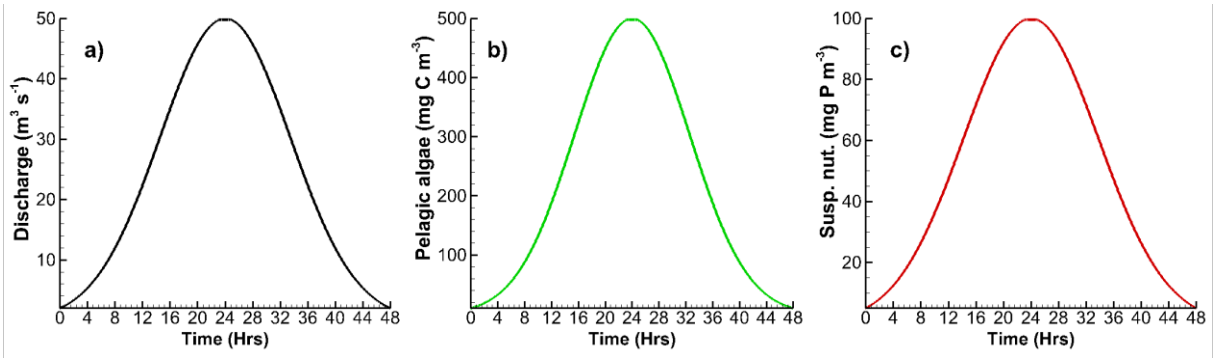

Fig. 10. Transient boundary condition for a) discharge, b) pelagic algae and c) suspended nutrients

discharge varying from 2 m^3 s^{-1} to 50 m^3 s^{-1}, pelagic algae varying from 10 to 500 mg C m^{-3} and suspended nutrients from 5 to 100 mg P m^{-3} in Gaussian fashion for the simulated time frame of 48 hrs with maximum values attained at the end of 24 hrs period (Figs. 10). It should be noted that the transient discharge will lead to transient half-reach residence time which will have a distinct bearing on the evolution of the major state variables.

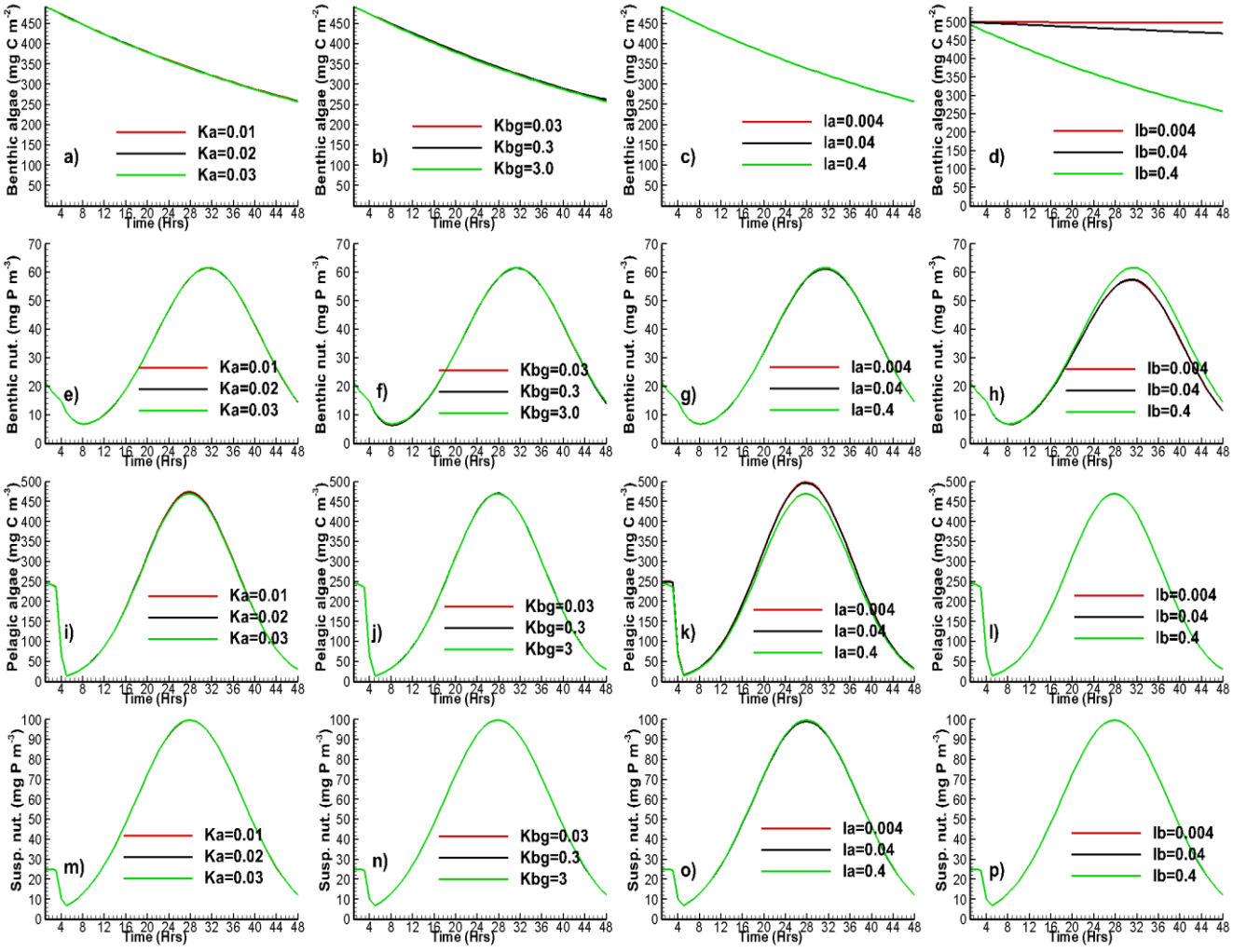

Fig. 11. Variation of benthic algae (a-d), benthic nutrients (e-h), pelagic algae (i-l) and suspended nutrients (m-p) at the midpoint of the stream, 15 kms from the upstream end, for transient flow, pelagic algae and suspended nutrient concentration at benthic algae entrainment rate (E) of 0.002 s m^{-1} day^{-1}

For the aforementioned transient boundary concentrations, the final concentration of benthic algae at the end of the simulation is around 260 mg C m^{-3} (Figs. 11 a-d) which is similar to the values obtained for both low flow scenario (Figs 6 a-d) and high flow scenario (Figs. 8 a-d).

This reaffirms the fact that the temporal evolution of benthic algae is insensitive to the upstream boundary concentration. The loss rate of benthic algae (lb) continues to be the most sensitive parameter and reducing the same successively by an order of magnitude (Fig. 11d) results in less depletion and higher concentration of algae in the benthic zone at the end of the simulation. As regard to the evolution of benthic nutrients, similar to the simulation of high flow scenario, the evolution is impacted by the upstream boundary concentration of suspended nutrients. However, till approximately time-mark of 8.5 hrs after the start of the simulation we observed continued decay in the concentration of benthic algae similar to low flow scenario. Beyond the aforementioned time mark the concentration of benthic nutrients is very similar to the Gaussian boundary prescribed for the suspended nutrients at the upstream end of the modelled domain. The cyclical and coupled nature of the evolution of benthic algae and benthic nutrients can be seen in Figs. 11d and 11h. Reduction of loss rate due benthic algae (lb) by order of magnitude leads to higher final concentration of benthic algae (Fig. 11 d red and black lines) which in turn results in lower peak nutrient concentration in the benthic zone (Fig. 11 h red and black lines). As regard to the evolution of pelagic algae and nutrients in the water column the temporal evolution is predominantly governed by the upstream boundary concentration beyond 4.5 hrs mark. However, before this time mark we see concomitant decrease in the concentration of pelagic algae and suspended nutrients. This decrease in the concentration of pelagic algae, during the aforementioned time frame, can be explained by the dominance of the parameter associated the with loss rate of pelagic algae (la) which depletes the concentration at the midpoint of the modelled domain before it gets influence by the boundary concentration after 4.5 hrs time mark. This decrease in pelagic algae combined with rapid loss of benthic nutrients leads to the domination of sink terms in the governing equation of suspended nutrients resulting in its loss too before the time mark of 4.5 hrs before it gets superseded by the boundary concentration coming from the upstream end of the domain.

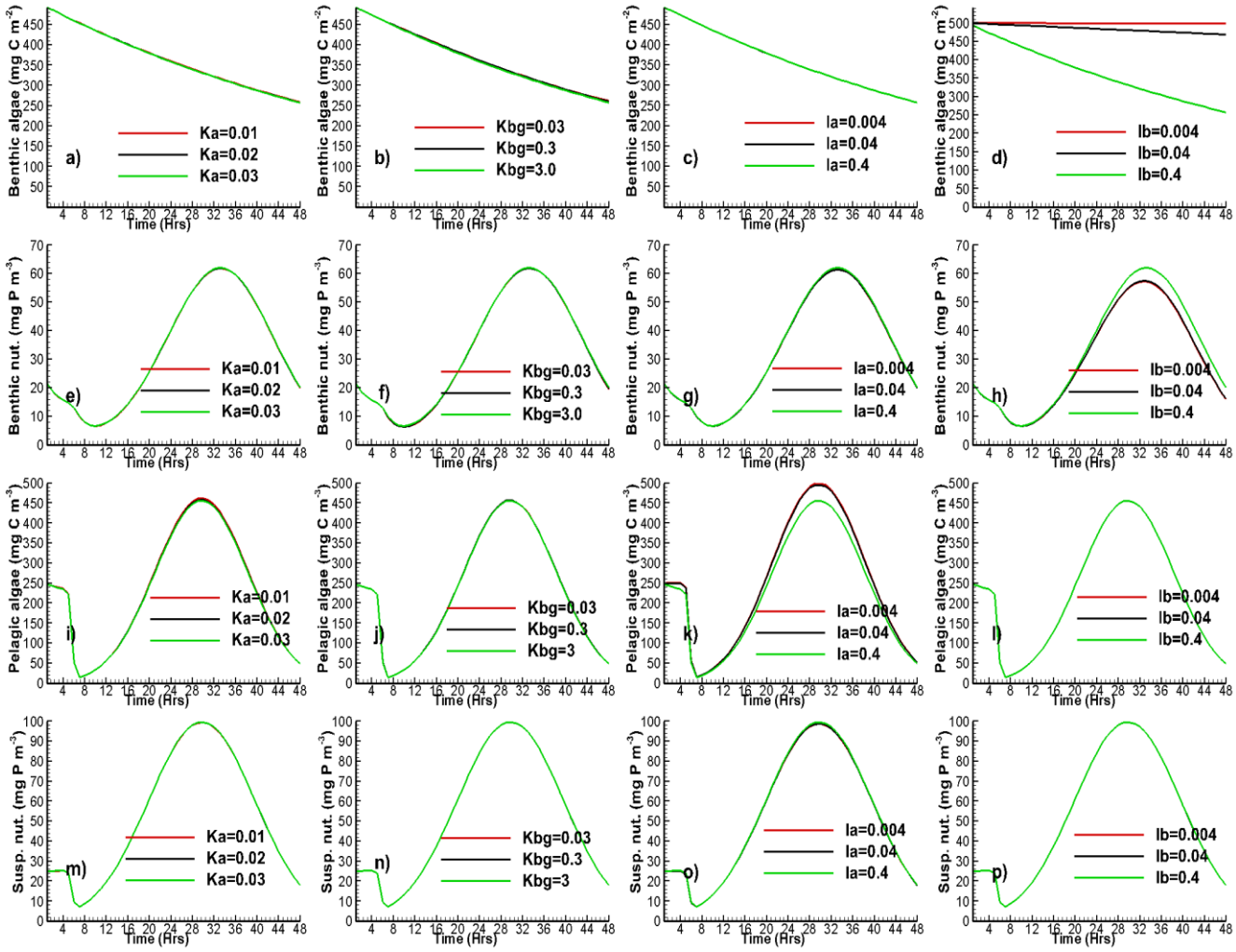

Fig. 12. Variation of benthic algae (a-d), benthic nutrients (e-h), pelagic algae (i-l) and suspended nutrients (m-p) at 22.5 kms from the upstream end of stream for transient flow, pelagic algae and suspended nutrient concentration at benthic algae entrainment rate (E) of 0.002 s m^{-1} day^{-1}

Our simulations consistently revealed the importance of the upstream boundary concentration, half-reach residence time and the constituents driven by advection in the system. In order to examine this further and because our model is spatially explicit, we tracked the evolution of the modelled state variables at 22.5 kms from the upstream end of the domain (Fig. 12). We observed the exactly same trends in the evolution of the major state variables, as observed in the middle of the domain, albeit shifted in time. As the water parcel starting at the upstream end of the domain takes longer to reach the 22.5 km mark, the biological processes happening can continue for longer period of time (Fig. 12) before getting superseded by the upstream boundary concentration.

5 Conclusion

In the research work presented in this paper, we developed a numerical model, first of its kind, to examine the spatiotemporal dynamics of suspended and benthic algae in concomitant fashion in a riverine ecosystem. The developed model, tracked the variation of algae and nutrients in longitudinal direction. The numerical scheme of the model was first validated with the analytical solution of the standard advection-dispersion-reaction (ADR) equation with linear as well as non-linear decay term. Model was finally applied to the 30 kms stretch of the Bode River in Central Germany. Simulations were conducted to explore the impact of changing flow rate, light intensity and different loss rates of suspended and benthic algae, on the temporal evolution of concentration of algae and nutrients in pelagic and benthic zone. The spatially explicit nature of the model enabled us to track the temporal variation of the modelled state variables at different spatial points in the river-reach simultaneously. This modelling approach is different from the methodology adopted by other researchers (Whitehead et al., 2015; Lazar et al., 2016) where the river reach is generally modelled as a single spatial unit. The numerical modelling exercise, presented here, provided an insight into the cause-effect relationship for the spatiotemporal variation of algae present in pelagic and benthic zone. Furthermore, the modelling exercise, showed the relative importance of different parameters in the temporal evolution of suspended and benthic algae. Our research emphasized the limitation of residence time on the biological activity. The loss rate of pelagic (la) and benthic algae (lb) was identified to be the most sensitive parameters affecting the temporal evolution of pelagic and benthic algae. However, largest uncertainty, stems from the possible big range in entrainment rate (E) of benthic algae from benthic to pelagic zone which warrants more research in lab as well as field. The model developed here could easily be extended to examine the impact of point loads distributed along the river reach and to identify its zone of influence.

As the operational field monitoring can be expensive, development and application of numerical models can be a viable alternative to study aquatic ecosystem, however, models of this kind needs extensive dataset for validation before its results can be used with confidence.

References

Allen, J.I., Smyth, T.J., Siddorn, J.R., Holt, M., 2008. How well can we forecast high biomass algal bloom events in a eutrophic coastal sea? Harmful Algae 8, 70e76.

Anita, A. N., 2005. Solubilization of particles in sediment traps: revisiting the stochiomentry of mixed layer export. Biogeosciences 2: 189-204

Brunner, G.W., 2010. HEC-RAS, River Analysis System Hydraulic Reference Manual (Version 4.1). Report CPD-69, US Army Corps of Engineers, Hydrologic Engineering Center (HEC), Davis California, USA, pp 441

Caraco N. J., and Likens G. 1992. New and recycled primary production in an oligotrophic lake – insights for summer phosphorus dynamics. Limnology and Oceanography, 37, pp 590-602

Chao X., Jia Y., Shields F. D., Wang S. S. Y. and Cooper C., M., 2008. Three-dimensional numerical modeling of cohesive sediment transport and wind wave impact in a shallow oxbow lake. Advances in Water Resources, 31, pp 1004 - 1014

Chapra S. C., 2008. Surface Water-Quality modeling. Waveland Press, Inc., Long Grove, IL

Chun, Y., X. Qiujin, K. Hainan, S. Zhemin, and Y. Changzhou (2007), Eutrophication conditions and ecological status in typical bays of Lake Taihu in China, Environmental Monitoring and Assessment 135, 217–225.

Cox BA. A review of dissolved oxygen modelling techniques for lowland rivers. Sci Total Environ 2003;314–316:303–34.

David, A. C., G. Marie-E've and S. Erica (2010). Harmful algae and their potential impacts on desalination operations off southern California, Water Research 44, 385–416.

Deng, Z., Singh, V. P. and Bengtsson, L. (2001). Longitudinal dispersion coefficients in straight rivers, Journal of Hydraulic Engineering V(127), No. (11).

Dodds, W.K., Bouska, W.W., Eitzmann, J.L., Pilger, T.J., Pitts, K.L., Riley, A.J., Schloesser, J.T., Thornbrugh, D.J., 2009. Eutrophication of U.S. freshwaters: analysis of potential economic damages. Environ. Sci. Technol. 43 (1), 12–19.

Dodds, W.K., Smith, V.H., Lohman, K., 2002. Nitrogen and phosphorus relationships to benthic algal biomass in temperate streams. Can. J. Fish. Aquat. Sci. 59 (5), 865–874.

Fischer, H. B., List, E. J., Koh, R.C.Y, Imberger, J., and Brooks, N. H., 1979. Mixing in Inland and Coastal Waters. Academic Press, San Diego, California 92101-4495

Flynn, K.F., Chapra, S.C., Suplee, M.W., 2013. Modeling the lateral variation of bottom-attached algae in rivers. Ecological Modellling 267,pp 11-25

Gao, Y., Zhang, Y., Zhang, Y., 2007. Effects of flow velocity on growth of Microcystis aeruginosa in Taihu Lake. Journal of Ecology and Rural Environment 23 (2), 57–60, 88.

Graba, M., F. Y. Moulin, S. Boulêtreau, F. Garabétian, A. Kettab, O. Eiff, J. M. Sánchez-Pérez, and S. Sauvage (2010), Effect of near-bed turbulence on chronic detachment of epilithic biofilm: Experimental and modeling approaches, Water Resour. Res., 46, W11531, doi:10.1029/2009WR008679.

Godunov, S., K., 1950. A difference scheme for the numerical solution of discontinuous solution of hydrodynamic equations. Matematicheski Sbornink 47, 271-303

Harten, A., 1983. High resolution schemes for hyperbolic conservation laws. Journal of Computational Physcics 49, 357-393

Heisler, J., Glibert, P.M., Burkholder, J.M., 2008. Eutrophication and harmful algal blooms: a scientific consensus. Harmful Algae 8, 3e13.

Henderson, F. M., 1966. Open Channel Flow. Macmillan Publishing Co. Inc

Huppert, A., Blasius, B., Olinky, R., Stone, L., 2005. A model for seasonal phytoplankton blooms. Journal of Theoretical Biology 236, 276e290.

Jager, C. G., Diehl, S., and Emans M., 2010. Physical determinants of phytoplankton production, algal stoichiometry and vertical nutrient fluxes. The American Naturalist V(175), No. (4).

Jager C. G. and Diehl S. 2014. Resource competition across habitat boundaries: asymmetric interactions between benthic and pelagic producers. Ecological Monographs. http://dx.doi.org/10.1890/13-0613.1

Kamjunke, N., Buttner, O., Jager, C. G., Marcus, H., Tumpling W. v., Helbedel, S., Norf, H., Brauns, M., Baborowski, M., Wild., R., Borchardt, D., Weitere, M. 2013. Biogeochemical patterns in a river network along a land use gradient. Environmental Monitoring Assessment V(185), 9221-9236

Kirk J. T. O., 1994. Light and photosynthesis in aquatic ecosystems. Cambridge University Press, Cambridge, UK.

Labiod, C., Godillot R., and Caussade, B., 2007. The relationship between stream periphyton dynamics and near-bed turbulence in rough open-channel flow. Ecological Modelling, 209, (2007) 78-96

Lazar, A.N., Wade, A.J., Moss, B. 2016. Modelling Primary Producer Interaction and Composition: an Example of a UK Lowland River. Environmental Modelling Assessment, 21, 125-148

Liang D., Wang X., Falconer R. A. and Bockelmann-Evans B. N. 2010. Solving the depth-integrated solute transport equation with a TVD-MacCormack scheme. Environmental Modelling & Software, 25, pp 1619-1629

Long, T., Wu, L., Meng, G., Guo, W., 2011. Numerical simulation for impacts of hydrodynamic conditions on algae growth in Chongqing Section of Jialing River, China. Ecological Modelling, 222, pp 112-119

Mitrovic, S.M., Oliver, R.L., Rees, C., 2003. Critical flow velocities for the growth and dominance of Anabaena circinalis in some turbid freshwater rivers. Freshwater Biology 48, 164–174

Peterson, M. L., Wakeham, S. G., Lee, C., Aseka M. A. and Miquel, J. C., 2005. Novel techniques for collection of sinking particles in the ocean and determining their settling rates. Limnology and Oceanography Methods 3:520-532

Pretty, J.N., Mason, C.F., Nedwell, D.B., Hine, R.E., Leaf, S., Dils, R., 2002. Environmental costs of freshwater eutrophication in England and Wales. Environ. Sci. Technol. 37 (2), 201–208.

Riley, G. A., Stommel, H., and Bumpus, D. F., 1949. Quantitative ecology of the plankton of the western North Atlantic. Bulletin of Bingham Oceanographic Collection of Yale University 12:1-169

Rizzo W., Lackey G. and Christian R. 1992. Significance of euphotic sediments to oxygen and nutrient cycling in a temperate estuary. Marine Ecology Progress Series,86, pp 51-61

Simon, E., Prochnik, James, U., Aurora, M., Nedelcu, et al., 2010. Genomic analysis of organismal complexity in the multicellular green alga Volvox carteri. Science 329, 223–226.

Sinha, S., Rode, M., and Borchardt, D., 2014.Evaluating a 1D and 2D water quality modelling framework: A case study of the lower Bode River Germany, EGU General Assembly, April 14^{th} – 16^{th}, 2014

Smil, V. (1999), Long-range perspectives on inorganic fertilizers in global agriculture, technical report, Int. Fert. Dev. Cent., Muscle Shoals, Ala.

Spalding, R. F., and M. E. Exner (1993), Occurrence of nitrate in groundwater a review, J. Environ. Qual., 22(3), 392–402.

Suplee, M.W., Watson, V., Dodds, W.K., Shirley, C., 2012. Response of algal biomass to large-scale nutrient controls in the Clark Fork River, Montana, United States. J. Am. Water Resources Association 48 (5), 1008-1021

Sverdrup, H. U. 1953. On conditions for the vertical blooming of phytoplankton. Journal du Conseil: Conseil Permanent International pour l'Exploration de la Mer 18:287-295

N. Muttil, J.H.W. Lee Genetic programming for analysis and real-time prediction of coastal algal blooms Ecol. Model., 189 (3–4) (2005), pp. 363–376

Vadeboncoeur Y., Lodge D. and Carpenter S. 2001. Whole-lake fertilization effects on distribution of primary production between benthic and pelagic habitats. Ecology, 82, pp 1065-1077

Valocchi, A.J., and Malmstead, M. 1992. Accuracy of operator splitting for advection dispersion reaction problems. Water Resources Research 28(5), pp 1471-1476

Wade, A.J., Hornberger, G.M., Whitehead, P.G., Jarvie, H.P., & Flynn, N. J. (2001). On modeling the mechanisms that control instream phosphorus, macrophyte and epiphyte dynamics: an assessment of a new model using general sensitivity analysis. Water Resources Research, 37(11), 2777-2792

Welch, E.B., Jacoby, J.M., Horner, R.R., Seeley, M.R., 1988. Nuisance biomass levels of periphytic algae in streams. Hydrobiologia 157 (2), 161-168

Whitehead, P. G., Bussi, G., Bowes, M. J., Read, D.S., Hutchins, M.G., Elliott, J. A., Dadson, S.J. 2015. Dynamic modelling of multiple phytoplankton groups in rivers with an application to the Thames river system in the UK. Environmental Modelling & Software, 74, (2015) 75-91

Whitehead, P.G., & Hornbrger, G.M.1984. Modelling algal behaviour in the River Thames. Water Resources, 18(8), 945-953

Yamamoto T, Hashimoto T, Tarutani K, Kotani Y. Effects of winds, tides and river water runoff on the formation and disappearance of the Alexandrium tamarense bloom in Hiroshima Bay, Japan. Harmful Algae. 2002. 1(3): 301-312.

Zacharias, S., Bogena, H., Samaniego, L., Mauder, M., Fus, R., Putz, T., Frenzel, M., Schwank, M., Baessler, C., Butterbach-Bahl, K., Bens, O., Borg, E., Brauer, A., Dietrich, P., Hajnsek, I., Helle, G., Kiese, R., Kunstmann, H., Klotz, S., Munch, J. C., Papen, H., Priesack, E., Schmid, H. P., Steinbrecher, R., Rosenbaum, U., Teutsch, G., and Vereecken, H. ,2011. A network of Terrestrial Environmental Observatories in Germany. Vadose Zone Journal 10, 955-973